PROCEEDINGS OF SCIENCE

Electroweak penguin decays at LHCb

Christoph Langenbruch[a,†,*]

[a] *RWTH Aachen University,*
I. Physikalisches Institut B, Sommerfeldstr. 14, 52056 Aachen, Germany

E-mail: christoph.langenbruch@cern.ch

Electroweak penguin decays proceed via favour changing neutral currents, which are heavily (loop-)suppressed in the Standard Model (SM). They therefore constitute sensitive probes for new heavy particles beyond the SM that can give significant virtual contributions. These contributions can modify branching fractions and angular observables of rare $b \to s\ell^+\ell^-$ decays. Recent measurements in this area have shown tensions with SM predictions, which are colloquially referred to as *flavour anomalies*. These proceedings discuss the status of the anomalies in rare $b \to s\mu^+\mu^-$ decays, focusing on the latest measurements by the LHCb collaboration.

**** The European Physical Society Conference on High Energy Physics (EPS-HEP2021), ****
**** 26-30 July 2021 ****
**** Online conference, jointly organized by Universität Hamburg and the research center DESY ****

*Speaker
†On behalf of the LHCb collaboration

PoS(EPS-HEP2021)561

1. Introduction

Electroweak penguin decays of b-hadrons proceed via flavour changing neutral currents and are therefore forbidden at the tree-level in the Standard Model (SM). At lowest perturbative order, rare $b \to s\ell^+\ell^-$ decays are allowed through penguin- and box-diagrams and are therefore both loop- and CKM-suppressed. They thus constitute rare processes, to which new, heavy particles in SM extensions can give significant virtual contributions. These contributions can change decay rates and rate asymmetries, as well as angular distributions of final state particles.

Several tensions with SM predictions have appeared in the area of rare $b \to s\ell^+\ell^-$ decays, most notably in measurements of branching fractions [1–5], angular analyses [6–9], and tests of lepton universality [10–13], for which particularly clean SM predictions are available. These proceedings discuss the most recent measurements of branching fractions and angular observables in $b \to s\mu^+\mu^-$ decays, with particular focus on the latest results from the LHCb collaboration.

2. Decay rates

Measurements of the branching fractions of $b \to s\mu^+\mu^-$ decays have been found to consistently lie below the SM predictions for $B^+ \to K^+\mu^+\mu^-$, $B^0 \to K^0_S\mu^+\mu^-$ [5], $B^0 \to K^{*0}\mu^+\mu^-$ [2], $B^+ \to K^{*+}\mu^+\mu^-$ [5] and $B^0_s \to \phi\mu^+\mu^-$ decays [1, 3]. These tensions range from 1–3 standard deviations (σ), depending on the decay mode and assumptions on the hadronic uncertainties of the SM prediction from non-perturbative form factor calculations and contributions from the so-called *charm-loop*.

2.1 $B^0_s \to \phi\mu^+\mu^-$

One of the most significant deviations is found for the branching fraction of the decay $B^0_s \to \phi\mu^+\mu^-$ [1, 3]. An analysis using the LHC Run 1 data found the branching fraction to be below the SM prediction at the level of $3\,\sigma$. Recently, an updated analysis using the full Run 1 and 2 data sample of the LHCb experiment, corresponding to an integrated luminosity of $9\,\mathrm{fb}^{-1}$, has been published [1]. The analysis reconstructs the decay using the final state $\phi(\to K^+K^-)\mu^+\mu^-$ and determines the $B^0_s \to \phi\mu^+\mu^-$ branching fraction in several ranges of q^2, the invariant mass of the dimuon system squared. The q^2 regions $8.0 < q^2 < 11.0\,\mathrm{GeV}^2/c^4$ and $12.5 < q^2 < 15.0\,\mathrm{GeV}^2/c^4$ contain the tree-level charmonium decays $B^0_s \to J/\psi(\to \mu^+\mu^-)\phi$ and $B^0_s \to \psi(2S)(\to \mu^+\mu^-)\phi$ which dominate the rare signal mode in these ranges and are therefore vetoed. These decays however constitute important control modes and the decay $B^0_s \to J/\psi\,\phi$ is used for normalisation. The differential branching fraction for the rare signal decay $B^0_s \to \phi\mu^+\mu^-$ in the q^2 range $[q^2_{\mathrm{min}}, q^2_{\mathrm{max}}]$ is calculated according to

$$\frac{\mathrm{d}\mathcal{B}(B^0_s \to \phi\mu^+\mu^-)}{\mathrm{d}q^2} = \frac{\mathcal{B}(B^0_s \to J/\psi\,\phi) \times \mathcal{B}(J/\psi \to \mu^+\mu^-)}{q^2_{\mathrm{max}} - q^2_{\mathrm{min}}} \times \frac{N_{\phi\mu^+\mu^-}}{N_{J/\psi\,\phi}} \times \frac{\epsilon_{J/\psi\,\phi}}{\epsilon_{\phi\mu^+\mu^-}}, \tag{1}$$

where $N_{\phi\mu\mu}$ and $N_{J/\psi\,\phi}$ denote the yields of signal and normalisation mode, and $\epsilon_{\phi\mu\mu}$ and $\epsilon_{J/\psi\,\phi}$ their respective efficiencies. As normalisation mode and signal decay have an identical final state, many experimental systematic effects cancel in the efficiency ratio. Figure 1 (left) shows the signal candidates integrated over q^2 and the different data taking periods. In total 2006 ± 53 signal candidates are found. Figure 1 (right) shows the differential branching fraction, overlaid with SM predictions from Light Cone Sum Rules (LCSRs) at low q^2 [14–16] and Lattice calculations

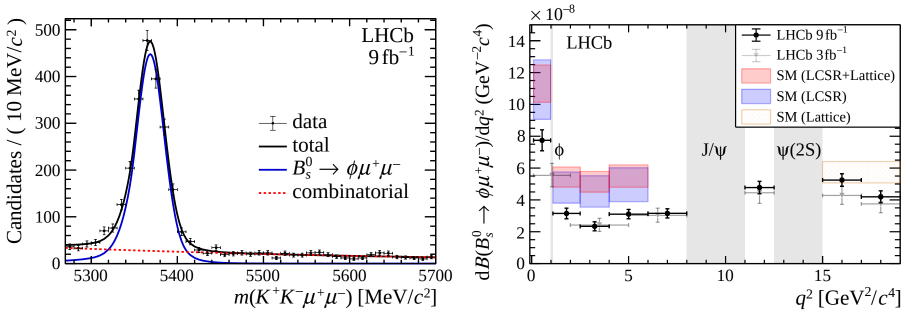

Figure 1: (Left) Reconstructed B_s^0 mass for $B_s^0 \to \phi\mu^+\mu^-$ signal candidates integrated over the full q^2 range $0.1 < q^2 < 18.9\,\text{GeV}^2/c^4$, overlaid with the fit projections. (Right) Differential branching fraction of the signal decay $B_s^0 \to \phi\mu^+\mu^-$, depending on q^2, overlaid with SM predictions [14–18].

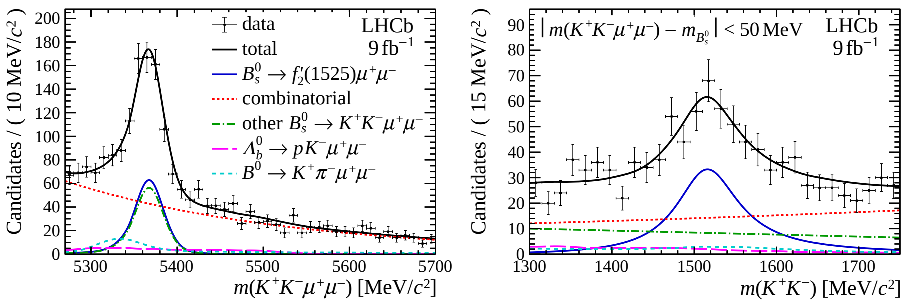

Figure 2: Reconstructed invariant mass of (left) the $K^+K^-\mu^+\mu^-$ system and (right) the K^+K^- system in the B_s^0 signal region $\pm 50\,\text{MeV}/c^2$ around the known B_s^0 mass, overlaid with the fit projections.

(LQCD) at high q^2 [17, 18]. In the q^2 range $1.1 < q^2 < 6.0\,\text{GeV}^2/c^4$, the differential branching fraction of $(2.88 \pm 0.22) \times 10^{-8}\,\text{GeV}^2/c^4$ is found to lie $3.6\,\sigma$ below a precise SM prediction of $(5.37 \pm 0.66) \times 10^{-8}\,\text{GeV}^2/c^4$ which uses a combination of LCSR and LQCD calculations. A less precise SM prediction of $(4.77 \pm 1.01) \times 10^{-8}\,\text{GeV}^2/c^4$ based on LCSRs alone lies $1.8\,\sigma$ above the measurement.

2.2 $B_s^0 \to f_2'(1525)\mu^+\mu^-$

In addition to the measurement of $B_s^0 \to \phi\mu^+\mu^-$, Ref. [1] also reports the first observation of the decay $B_s^0 \to f_2'(1525)(\to K^+K^-)\mu^+\mu^-$. A two-dimensional fit in the reconstructed invariant mass of the $K^+K^-\mu^+\mu^-$ and the K^+K^- system is performed to separate the f_2' signal from S- and P-wave contributions. Figure 2 shows the signal candidates, overlaid with the fit projections. Integrated over q^2 the fit finds 290 ± 36 signal candidates in total. The statistical significance of the signal, determined using Wilks' theorem, is found to be $9\,\sigma$. The total branching fraction is determined to be $\mathcal{B}(B_s^0 \to f_2\mu^+\mu^-) = (1.57 \pm 0.19 \pm 0.12) \times 10^{-7}$, in agreement with SM predictions [19–21].

3. Angular analyses

3.1 $B^0 \to K^{*0}\mu^+\mu^-$

The rare decay $B^0 \to K^{*0}(\to K^+\pi^-)\mu^+\mu^-$ allows access to many angular observables sensitive to New Physics (NP) contributions. The *CP*-averaged differential decay rate in a bin of q^2, and

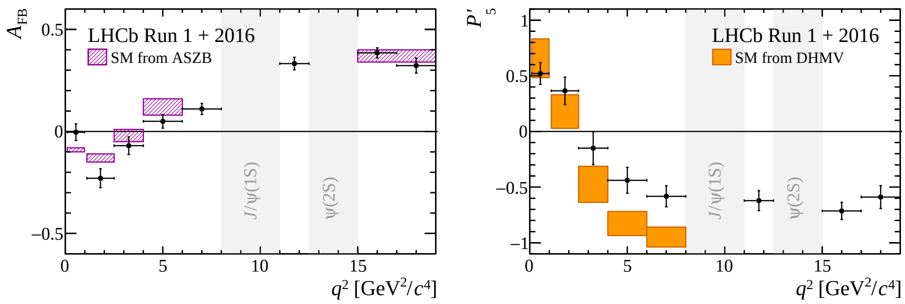

Figure 3: (Left) Forward-backward asymmetry $A_{\rm FB}$ and (right) less form-factor dependent observable P'_5 from the decay $B^0 \to K^{*0}\mu^+\mu^-$ [8], together with SM predictions from Refs. [14, 15, 24, 25].

depending on the three decay angles $\cos\theta_\ell$, $\cos\theta_K$ and ϕ, is given by [22]

$$\begin{aligned}\frac{1}{\mathrm{d}(\Gamma+\bar{\Gamma})/\mathrm{d}q^2}\frac{\mathrm{d}^3(\Gamma+\bar{\Gamma})}{\mathrm{d}\cos\theta_\ell\mathrm{d}\cos\theta_K\mathrm{d}\phi} = \frac{9}{32\pi}\Big[&\tfrac{3}{4}(1-F_{\rm L})\sin^2\theta_K + F_{\rm L}\cos^2\theta_K + \tfrac{1}{4}(1-F_{\rm L})\sin^2\theta_K\cos 2\theta_\ell \\ &- F_{\rm L}\cos^2\theta_K\cos 2\theta_\ell + S_3\sin^2\theta_K\sin^2\theta_\ell\cos 2\phi \\ &+ S_4\sin 2\theta_K\sin 2\theta_\ell\cos\phi + S_5\sin 2\theta_K\sin\theta_\ell\cos\phi \\ &+ \tfrac{4}{3}A_{\rm FB}\sin^2\theta_K\cos\theta_\ell + S_7\sin 2\theta_K\sin\theta_\ell\sin\phi \\ &+ S_8\sin 2\theta_K\sin 2\theta_\ell\sin\phi + S_9\sin^2\theta_K\sin^2\theta_\ell\sin 2\phi\Big]. \qquad (2)\end{aligned}$$

Here, $F_{\rm L}$ denotes the longitudinal polarisation fraction, and $A_{\rm FB}$ the forward-backward asymmetry. The LHCb collaboration has measured the full set of angular observables using the Run 1 and 2016 data sample corresponding to an integrated luminosity of $4.7\,\mathrm{fb}^{-1}$ [8]. In addition, the LHCb collaboration has also determined the less form-factor dependent observables $P_i^{(\prime)}$, proposed in Ref. [23], for which the hadronic form factor uncertainties cancel at leading order. Figure 3 shows the observable $A_{\rm FB}$ and $P'_5 = S_5/\sqrt{F_{\rm L}(1-F_{\rm L})}$, together with SM predictions from Refs. [14, 15, 24, 25]. In the q^2 regions $4 < q^2 < 6\,\mathrm{GeV}^2/c^4$ and $6 < q^2 < 8\,\mathrm{GeV}^2/c^4$ local tensions with the SM prediction corresponding 2.5 and 2.9 σ are found for the observable P'_5. The global significance of the tension is found to correspond to 3.3 σ, depending on the q^2 range used and assumptions on hadronic uncertainties [8].

3.2 $B^+ \to K^{*+}\mu^+\mu^-$

The decay $B^+ \to K^{*+}\mu^+\mu^-$ is the isospin partner of the mode $B^0 \to K^{*0}\mu^+\mu^-$ and allows access to the same angular observables. The LHCb collaboration has performed the first measurement of the full set of *CP*-averaged angular observables using the full Run 1 and 2 data sample, corresponding to $9\,\mathrm{fb}^{-1}$ [7]. The K^{*+} meson is reconstructed in the $K^0_{\rm S}(\to\pi^+\pi^-)\pi^+$ final state. Figure 4 shows the resulting angular observables $P_2 = \frac{2}{3}A_{\rm FB}/(1-F_{\rm L})$ and P'_5, overlaid with SM predictions from Refs. [14, 15, 17, 18, 25–27]. The largest local discrepancy with the SM prediction is found for P_2 in the q^2 range $6 < q^2 < 8\,\mathrm{GeV}^2/c^4$, corresponding to 3.0 σ. Overall, the pattern of deviations in P_2 ($A_{\rm FB}$) and P'_5 broadly agrees with the tensions observed in $B^0 \to K^{*0}\mu^+\mu^-$.

PoS(EPS-HEP2021)561

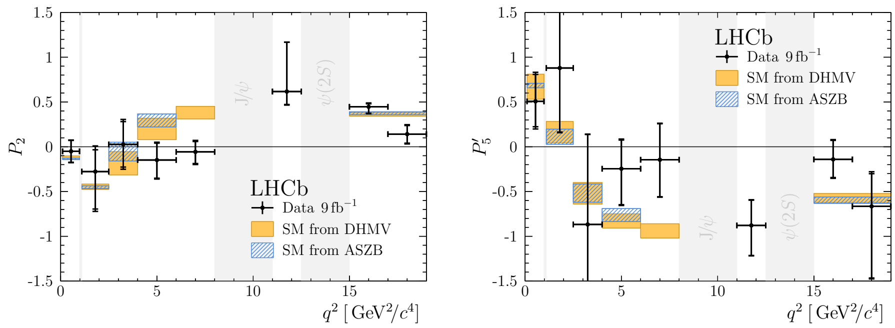

Figure 4: Angular observables with reduced form-factor dependence(left) $P_2 = \frac{2}{3}A_{\rm FB}/(1 - F_{\rm L})$ and (right) P_5' determined using the decay $B^+ \to K^{*+}\mu^+\mu^-$ [7], overlaid with SM predictions [14, 15, 17, 18, 25–27].

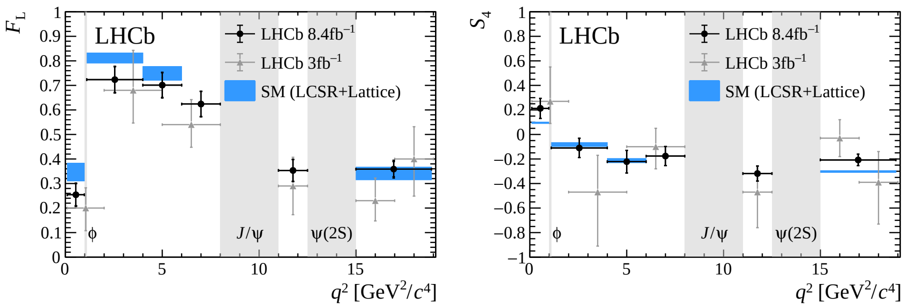

Figure 5: *CP*-averaged angular observables $F_{\rm L}$ and S_4 from the rare decay $B^0_s \to \phi\mu^+\mu^-$ [6], overlaid with SM predictions [14, 16–18].

3.3 $B^0_s \to \phi\mu^+\mu^-$

In contrast to the decays $B^0 \to K^{*0}\mu^+\mu^-$ and $B^+ \to K^{*+}\mu^+\mu^-$, the final state of the decay $B^0_s \to \phi(\to K^+K^-)\mu^+\mu^-$ is not flavour-specific. In an untagged angular analysis only a reduced set of observables is therefore accessible; the *CP*-averaged observables $F_{\rm L}$ and $S_{3,4,7}$, and the *CP*-asymmetries $A^{CP}_{\rm FB}$ and $A_{5,8,9}$ (which replace the observables $A_{\rm FB}$ and $S_{5,8,9}$ in Eq. 2). The LHCb collaboration has recently performed an updated angular analysis using data corresponding to an integrated luminosity of 8.4 fb^{-1} [6]. The *CP*-averaged observables $F_{\rm L}$ and S_4 are shown in Fig. 5. Overall good agreement with the SM predictions [14, 16–18] is found, with some mild tension in $F_{\rm L}$ at low q^2. The *CP*-asymmetries are found to be consistent with zero, in good agreement with the SM expectation.

4. Interpretation

Experimental data on rare $b \to s\mu^+\mu^-$ decays can be interpreted in the framework of effective field theory. The angular observables discussed in these proceedings can be used to determine the effective $b \to s\ell^+\ell^-$ couplings, the *Wilson coefficients*. For the angular analyses of the decays $B^0 \to K^{*0}\mu^+\mu^-$, $B^+ \to K^{*+}\mu^+\mu^-$ and $B^0_s \to \phi\mu^+\mu^-$ the FLAVIO flavour software [16] is used to determine the Wilson coefficient $\mathcal{R}e(C_9)$, the $bs\mu\mu$ vector-coupling. Figure 6 shows the resulting shift of $\mathcal{R}e(C_9)$ from its SM value. The measurements result in a consistent negative shift of $\mathcal{R}e(C_9)$,

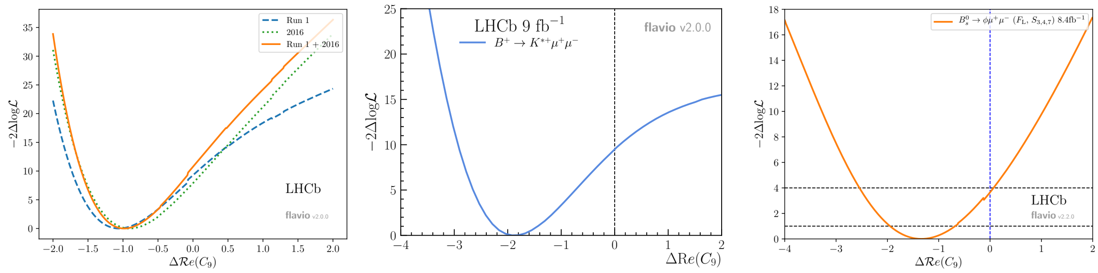

Figure 6: Fit of a shift of the Wilson coefficient $\mathcal{R}e(C_9)$ from its SM value using the angular observables from the decays (left) $B^0\to K^{*0}\mu^+\mu^-$, (centre) $B^+\to K^{*+}\mu^+\mu^-$, and (right) $B_s^0\to\phi\mu^+\mu^-$ [6–8] using the FLAVIO flavour software [16].

which is preferred over the SM hypothesis by 2–3 σ. It should be noted that the significance of the tensions depends on assumption on hadronic uncertainties due to the contribution from the charm-loop, which are currently under discussion [28–32]. Combining all available experimental data on $b\to s\mu^+\mu^-$ transitions with measurements of the theoretically clean lepton universality tests results in tensions corresponding to 5–6 σ [33–35]. Consistent NP explanations of the *flavour anomalies* in rare decays are available for example in the form of new heavy gauge bosons (*e.g.* Refs. [36–39]) and leptoquarks (*e.g.* Refs. [40–43]).

5. Conclusions

Recent measurements of branching fractions and angular observables in $b\to s\mu^+\mu^-$ decays presented in these proceedings have shown tensions with SM predictions. Together with the tests of lepton universality in $b\to s\ell^+\ell^-$ transitions these tensions constitute the *flavour anomalies* in rare decays. Consistent interpretations of the anomalies in the framework of effective field theory are possible and several potential explanations in the terms of NP models have been proposed.

The experimental measurements in rare *b*-hadron decays are generally statistically dominated. The large data samples that will be available in the LHCb upgrade(s) will therefore allow for unprecedented precision in the measurements of $b\to s\ell^+\ell^-$ decays. Independent clarification of the anomalies is also expected from future measurements by the Belle II experiment.

Acknowledgements

C. L. gratefully acknowledges support by the Emmy Noether programme of the Deutsche Forschungsgemeinschaft (DFG), grant identifier LA 3937/1-1.

References

[1] LHCb collaboration, *Phys. Rev. Lett.* **127** (2021) 151801 [arXiv:2105.14007].

[2] LHCb collaboration, *JHEP* **11** (2016) 047 [arXiv:1606.04731].

[3] LHCb collaboration, *JHEP* **09** (2015) 179 [arXiv:1506.08777].

[4] LHCb collaboration, *JHEP* **06** (2015) 115 [arXiv:1503.07138].

[5] LHCb collaboration, *JHEP* **06** (2014) 133 [arXiv:1403.8044].

[6] LHCb collaboration, [arXiv:2107.13428].

[7] LHCb collaboration, *Phys. Rev. Lett.* **126** (2021) 161802 [arXiv:2012.13241].

[8] LHCb collaboration, *Phys. Rev. Lett.* **125** (2020) 011802 [arXiv:2003.04831].

[9] LHCb collaboration, *JHEP* **02** (2016) 104 [arXiv:1512.04442].

[10] LHCb collaboration, [arXiv:2103.11769].

[11] LHCb collaboration, *Phys. Rev. Lett.* **122** (2019) 191801 [arXiv:1903.09252].

[12] LHCb collaboration, *JHEP* **05** (2020) 040 [arXiv:1912.08139].

[13] LHCb collaboration, *JHEP* **08** (2017) 055 [arXiv:1705.05802].

[14] A. Bharucha, D.M. Straub and R. Zwicky, *JHEP* **08** (2016) 098 [arXiv:1503.05534].

[15] W. Altmannshofer and D.M. Straub, *Eur. Phys. J. C* **75** (2015) 382 [arXiv:1411.3161].

[16] D.M. Straub, [arXiv:1810.08132].

[17] R.R. Horgan, Z. Liu, S. Meinel and M. Wingate, *Phys. Rev. Lett.* **112** (2014) 212003 [arXiv:1310.3887].

[18] R.R. Horgan, Z. Liu, S. Meinel and M. Wingate, *PoS* **LATTICE2014** (2015) 372 [arXiv:1501.00367].

[19] Y.-B. Zuo, C.-X. Yue, B. Yu, Y.-H. Kou, Y. Chen and W. Ling, *Eur. Phys. J. C* **81** (2021) 30.

[20] N. Rajeev, N. Sahoo and R. Dutta, *Phys. Rev. D* **103** (2021) 095007 [arXiv:2009.06213].

[21] R.-H. Li, C.-D. Lu and W. Wang, *Phys. Rev. D* **83** (2011) 034034 [arXiv:1012.2129].

[22] W. Altmannshofer, P. Ball, A. Bharucha, A.J. Buras, D.M. Straub and M. Wick, *JHEP* **01** (2009) 019 [arXiv:0811.1214].

[23] S. Descotes-Genon, J. Matias, M. Ramon and J. Virto, *JHEP* **01** (2013) 048 [arXiv:1207.2753].

[24] S. Descotes-Genon, L. Hofer, J. Matias and J. Virto, *JHEP* **12** (2014) 125 [arXiv:1407.8526].

[25] A. Khodjamirian, T. Mannel, A.A. Pivovarov and Y.M. Wang, *JHEP* **09** (2010) 089 [arXiv:1006.4945].

[26] S. Descotes-Genon, L. Hofer, J. Matias and J. Virto, *JHEP* **06** (2016) 092 [arXiv:1510.04239].

[27] B. Capdevila, A. Crivellin, S. Descotes-Genon, J. Matias and J. Virto, *JHEP* **01** (2018) 093 [arXiv:1704.05340].

[28] S. Jäger and J. Martin Camalich, *Phys. Rev. D* **93** (2016) 014028 [arXiv:1412.3183].

[29] J. Lyon and R. Zwicky, [arXiv:1406.0566].

[30] M. Ciuchini, M. Fedele, E. Franco, S. Mishima, A. Paul, L. Silvestrini et al., *JHEP* **06** (2016) 116 [arXiv:1512.07157].

[31] M. Ciuchini, A.M. Coutinho, M. Fedele, E. Franco, A. Paul, L. Silvestrini et al., *Eur. Phys. J. C* **77** (2017) 688 [arXiv:1704.05447].

[32] N. Gubernari, D. van Dyk and J. Virto, *JHEP* **02** (2021) 088 [arXiv:2011.09813].

[33] M. Algueró, B. Capdevila, S. Descotes-Genon, J. Matias and M. Novoa-Brunet, in *55th Rencontres de Moriond on QCD and High Energy Interactions*, 4, 2021 [arXiv:2104.08921].

[34] W. Altmannshofer and P. Stangl, [arXiv:2103.13370].

[35] T. Hurth, F. Mahmoudi, D.M. Santos and S. Neshatpour, [arXiv:2104.10058].

[36] W. Altmannshofer, S. Gori, M. Pospelov and I. Yavin, *Phys. Rev. D* **89** (2014) 095033 [arXiv:1403.1269].

[37] A. Crivellin, G. D'Ambrosio and J. Heeck, *Phys. Rev. Lett.* **114** (2015) 151801 [arXiv:1501.00993].

[38] A. Celis, J. Fuentes-Martin, M. Jung and H. Serodio, *Phys. Rev. D* **92** (2015) 015007 [arXiv:1505.03079].

[39] A. Falkowski, M. Nardecchia and R. Ziegler, *JHEP* **11** (2015) 173 [arXiv:1509.01249].

[40] G. Hiller and M. Schmaltz, *Phys. Rev. D* **90** (2014) 054014 [arXiv:1408.1627].

[41] B. Gripaios, M. Nardecchia and S.A. Renner, *JHEP* **05** (2015) 006 [arXiv:1412.1791].

[42] I. de Medeiros Varzielas and G. Hiller, *JHEP* **06** (2015) 072 [arXiv:1503.01084].

[43] R. Barbieri, C.W. Murphy and F. Senia, *Eur. Phys. J. C* **77** (2017) 8 [arXiv:1611.04930].